Surface and interfacial tensions of Hofmeister electrolytes

Alexandre P. dos Santos and Yan Levin*

Received 9th April 2012, Accepted 25th April 2012
DOI: 10.1039/c2fd20067h

We present a theory that is able to account quantitatively for the surface and interfacial tensions of different electrolyte solutions. It is found that near the interface, ions can be separated into two classes: the kosmotropes and the chaotropes. While the kosmotropes remain hydrated near the interface and are repelled from it, the chaotropes loose their hydration sheath and become adsorbed to the surface. The anionic adsorption is strongly correlated with the Jones–Dole viscosity *B*-coefficient. Both hydration and polarizability must be taken into account to obtain a quantitative agreement with the experiments. To calculate the excess interfacial tension of the oil–electrolyte interface, the dispersion interactions must also be included. The theory can also be used to calculate the surface and the interfacial tensions of acid solutions, predicting a strong surface adsorption of hydronium ion.

Introduction

Understanding the behavior of ions at the air–water and oil–water interfaces should help shed light on how the ions interact with proteins and colloidal particles. Over a hundred years ago Hofmeister organized various electrolytes according to their ability to salt-out protein solutions. The sequences of anions and cations, which now bear his name, have been also observed in the fields of science as diverse as biophysics, biochemistry, electro-chemistry and colloidal science.[1–5]

Although the bulk thermodynamics of electrolyte solutions is fairly well understood,[6] we still know little about ionic behavior when the translational symmetry is broken.[7–11] The surface and the interfacial tensions provide us with an indirect indication of ionic distribution near an interface. A long time ago Heydweiller[12] observed that addition of salt increases the surface tension of the air–water interface. Heydweiller also noted that the effect of different electrolytes followed the sequence found by Hofmeister some years earlier. The increase of the surface tension by electrolytes was soon attributed to the ionic depletion from the interfacial region.[7] Wagner[8] and Onsager and Samaras[9] suggested that this was a consequence of the charge induced on the dielectric interface separating water from air. The theory was able to quantitatively account for the surface tension of sodium chloride solution at very large dilutions, but failed for larger concentrations of electrolyte. Inclusion of ionic hydration into the theory by Levin and Flores-Mena[10] extended its validity up to 1 M concentration. However when the same theory was applied to study the surface tension of sodium iodide solutions it was found that it predicted a qualitatively incorrect behavior—the surface tension of NaI was found to be larger than of NaCl, contrary to the experiments. The origin of this discrepancy was not clear. The fundamental insights, however, appeared soon after in the form of polarizable force fields simulations[13–19] and

Instituto de Física, Universidade Federal do Rio Grande do Sul, Caixa Postal 15051, CEP 91501-970 Porto Alegre, RS, Brazil. E-mail: levin@if.ufrgs.br

experiments.[20–22] The new simulations and experiments demonstrated that it was possible for large halogen anions to become adsorbed to the interface. The physical mechanism of this adsorption, however, remained unclear. Boström *et al.*[11] suggested that the dispersion (van der Waals) interactions, neglected within the Wagner–Onsager–Samaras (WOS) theory, were responsible for the ionic adsorption. This interesting suggestion, however, contradicts both experiments and simulations. Dispersion forces are proportional to the ionic polarizability. Therefore, strong dispersion interactions between ions and water should favor bulk solvation. Since anions are much more polarizable than cations, the dispersion interactions should want to keep these ions in the bulk, away from the interface. This means that a theory based on dispersion forces will predict that weakly polarizable cation might be adsorbed at the interface, contrary to what was found in experiments and simulations.

A different theory was recently advanced by Levin *et al.*[23,24] These authors argued that the driving force behind the adsorption of highly polarizable anions was due to the hydrophobic effect. To solvate an ion, a cavity must be created. The cavity perturbs the hydrogen bond network of water molecules, resulting in a free energy cost. Clearly if the ion moves towards the interface, the cavitational energy will diminish. There is, however, an electrostatic self-energy penalty of exposing the ionic charge to the low dielectric air environment. For hard, non-polarizable, ions of the WOS theory the self-energy penalty completely overwhelms the gain in the hydrophobic free energy, forcing these ions to remain in the bulk. The situation is very different for large polarizable anions. When such ions move towards the interface, their electronic charge distribution shifts so that it remains mostly hydrated. This drastically diminishes the electrostatic self-energy penalty of having such ions located at the interface. A careful calculation shows that for highly polarizable ions the electrostatic self-energy penalty becomes comparable to the gain in the hydrophobic free energy resulting from moving an ion from the bulk to the surface.[23]

In this paper we will show how the ideas presented above can be used to calculate the surface and the interfacial tensions of electrolytes and acid solutions, as well as their electrostatic potential difference across the dielectric interface.

The drop model

To perform the electrostatic calculations it is convenient to consider an electrolyte solution inside a spherical water drop of radius R.[24,25] Here we will choose $R =$ 300 Å, which is sufficiently large to avoid all finite size effects so that the excess surface tension calculated inside the drop will be the same as the surface tension of an extended thermodynamic interface. Outside the drop there is a low dielectric medium (air or oil), so that the interface at $r = R$ corresponds to the Gibbs dividing surface (GDS). N salt or acid "molecules" are dissociated inside the drop, resulting in N cations and N anions of charge $+q$ and $-q$, respectively. In the case of divalent anions, for each anion of charge $-2q$ there will be 2 cations of charge $+q$. The water and the external medium will be treated as dielectrics of permittivities ε_w and ε_o, respectively. The Bjerrum length is defined as $\lambda_B = \beta q^2/\varepsilon_w$.

The interfacial tensions are calculated by integrating the Gibbs adsorption isotherm equation,

$$d\gamma = -\Gamma_+ d\mu_+ - \Gamma_- d\mu_-, \tag{1}$$

where $\Gamma_\pm = [N - V\rho_\pm(0)]/S$ are the ionic excess due to interface, $\mu_\pm$ are the ionic chemical potentials, $\rho_\pm(0)$ are the ionic bulk concentrations, and S and V are the surface and the volume of the drop, respectively. The bulk concentrations are obtained from the numerical solution of the modified Poisson–Boltzmann (PB) equation:

$$\nabla^2\phi(r) = -\frac{4\pi q}{\varepsilon_w}\left[\rho_+(r) - \rho_-(r)\right],$$
$$\rho_\pm(r) = A_\pm e^{\left[\mp\beta q\phi(r) - \beta U_\pm(r)\right]},$$
$$A_\pm = N\Big/\left[4\pi\int_0^{r_{\max}} \mathrm{d}r\, r^2 e^{\left[\mp\beta q\phi(r) - \beta U_\pm(r)\right]}\right], \quad (2)$$

where $\phi(r)$ is the electrostatic potential, $\rho_\pm(r)$ are the ionic concentrations, and $r_{\max}$ is the maximum ionic distance from the center of the drop. For chaotropes $r_{\max} = R + a$ and for kosmotropes $r_{\max} = R - a$. The ion-interface interaction potentials, $U_\pm(r)$, will be discussed in the following sections. The chemical potentials inside the drop are constant and within the PB approximation are given by $\beta\mu_\pm = \log(\Lambda_\pm^3\rho_\pm(0))$, where $\Lambda_\pm$ are the thermal de Broglie wavelengths.

Air–water interface

When an ion moves close to the dielectric interface, there are two effects: (1) the interface becomes polarized; and (2) there is a loss of solvation free energy arising from the imperfect screening of the ionic electric field by the rest of electrolyte. Both of these effects lead to a repulsive force from the interface. The work necessary to bring an ion from the bulk to a distance z from the GDS is found to be[10,26]

$$\beta U_i(z) = \beta W\frac{a}{z}e^{-2\kappa(z-a)}, \quad (3)$$

where $\kappa = \sqrt{8\pi\lambda_B\rho(0)_\pm}$ is the inverse Debye length and a is the ionic radius. The contact value, W, is calculated by solving the Poisson equation with the appropriate boundary conditions,[10]

$$\beta W = \frac{\lambda_B}{2}\int_0^\infty \mathrm{d}p\frac{p\left[s\cosh(pa) - p\sinh(pa)\right]}{s\left[s\cosh(pa) + p\sinh(pa)\right]}, \quad (4)$$

where

$$s = \sqrt{\kappa^2 + p^2}.$$

For polarizable ions, Levin[23] calculated the variation in the electrostatic self-energy as an ion crosses the dielectric interface. The ion was modeled as an imperfect conducting sphere of relative polarizability $\alpha = \gamma_i/a^3$, where γ_i is the absolute ionic polarizability measured in $\mathrm{\AA}^3$. The electrostatic self-energy of an ion whose center is at distance $-a < z < a$ from the GDS is found to be

$$\beta U_p(z) = \frac{\lambda_B}{2a}\left[\frac{\pi x^2}{\theta(z)} + \frac{\pi[1-x]^2\varepsilon_w}{[\pi - \theta(z)]\varepsilon_o}\right] + g\left[x - \frac{1-\cos\left[\theta(z)\right]}{2}\right]^2, \quad (5)$$

where $\theta(z) = \arccos[-z/a]$ and $g = (1-\alpha)/\alpha$. The fraction of charge that remains hydrated x, is obtained by minimizing eqn (5),

$$x(z) = \left[\frac{\lambda_B\pi\varepsilon_w}{a\varepsilon_o\left[\pi - \theta(z)\right]} + g\left[1 - cos\left[\theta(z)\right]\right]\right]\Big/\left[\frac{\lambda_B\pi}{a\theta(z)} + \frac{\lambda_B\pi\varepsilon_w}{a\varepsilon_o\left[\pi - \theta(z)\right]} + 2g\right]. \quad (6)$$

To solvate an ion in water requires creation of a cavity. For small cavities this hydrophobic free energy scales with the volume of the void.[27] When the ion crosses the GDS, the perturbation to the hydrogen bond network diminishes, resulting in

a thermodynamic force that drives the ion towards the air–water interface. The cavitational potential energy is found to be

$$\beta U_c(z) = \begin{cases} va^3 \text{ for } z \geq a, \\ \dfrac{1}{4} va^3 \left(\dfrac{z}{a} + 1\right)^2 \left(2 - \dfrac{z}{a}\right) \text{ for } -a < z < a, \end{cases} \tag{7}$$

where $v \approx 0.3/\text{Å}^3$ is obtained using the bulk simulations.[27]

Physical chemists have known for a long time that ions come in two categories: structure-makers (kosmotropes) and structure-breakers (chaotropes). The separation into these two classes is often based on the Jones–Dole (JD) viscosity *B*-coefficient[28] which also correlates well with the ionic enthalpy of hydration.[29] In 1929 Jones and Dole observed that the relative viscosity η_r of an electrolyte solution is very well fitted by a simple formula $\eta_r = 1 + A\sqrt{c} + Bc$, where c is the bulk concentration of electrolyte. The square root term is universal and can be calculated using the Debye–Hückel–Onsager theory. On the other hand, the linear term in c is electrolyte specific. Ions with a positive *B* coefficient (kosmotropes) are supposed to organize water making it "more" viscous, while the ions with negative *B* are supposed to make water more disordered and "less" viscous. To what extent this physical picture is realistic is not clear, and recent experiments suggest that the action of ions on water molecules is much more local, not extending much beyond the first hydration shell.[30] This also agrees well with the theory of surface tensions of electrolyte solutions that will be presented in the present paper. We find that kosmotropic ions remain strongly hydrated near the interface and are repelled from it, while the chaotropic ions loose their hydration sheath and as the result of their large polarizability become adsorbed to the interface.

In the case of halides, the separations into kosmotropes and the chaotropes correlates well with the ionic size. Heavy halogen anions produce a weak electric field which is not sufficient to bind strongly the adjacent water molecules and prevent them from dissociating when a chaotropic ion approaches the interface. This is the case for I^- and Br^-, whose JD viscosity *B*-coefficients are -0.073 and -0.033, respectively. On the other hand, the small fluoride anion has large positive *B*-coefficient equal to 0.107. This ion, should therefore, remain strongly hydrated near a hydrophobic interface. The chloride ion, with a *B*-coefficient close to zero, -0.005, is on the borderline between the two classes.

The total interaction potential for strongly hydrated kosmotropes is dominated by the charge–image interaction, $U_\pm(z) = U_i(z)$ and the hard core repulsion (at one hydrated radius) from the GDS. On the other hand, large chaotropic anions, such as iodide and bromide, are able to cross the GDS with a relatively small electrostatic self-energy penalty, gaining the hydrophobic cavitational free energy. For such chaotropic anions the total ion–interface interaction potential is $U_-(z) = U_i(z) + U_p(z) + U_c(z)$. The radius[31] of I^- is $a = 2.26$ Å and its relative polarizability[32] is $\alpha = 0.64$; for Br^-, $a = 2.05$ Å and $\alpha = 0.59$.

The partially hydrated radius of the sodium cation Na^+ is the only free adjustable parameter of the theory. It is obtained by fitting the surface tension of the NaI solution. The calculation is performed by first numerically solving the PB equation to obtain the bulk concentration of electrolyte $\rho_\pm(0)$ at the center of the drop. Then, the Gibbs adsorption isotherm eqn (1) is integrated numerically to calculate the excess surface tension of the electrolyte solution. We find that $a = 2.5$ Å for Na^+ gives an excellent fit to the experimental data,[24] Fig. 1. The same radius of Na^+ is then used to calculate the excess surface tensions of other electrolyte solutions. Note that while Br^- is a chaotrope, both F^- and Cl^- are kosmotropes. Furthermore, for F^- the JD viscosity *B*-coefficient is large and positive while for Cl^- it is almost zero. Therefore near the interface, F^- will remain fully hydrated with the effective radius[33] $a = 3.52$ Å, while Cl^- is very weakly hydrated, with the radius $a = 2$ Å close

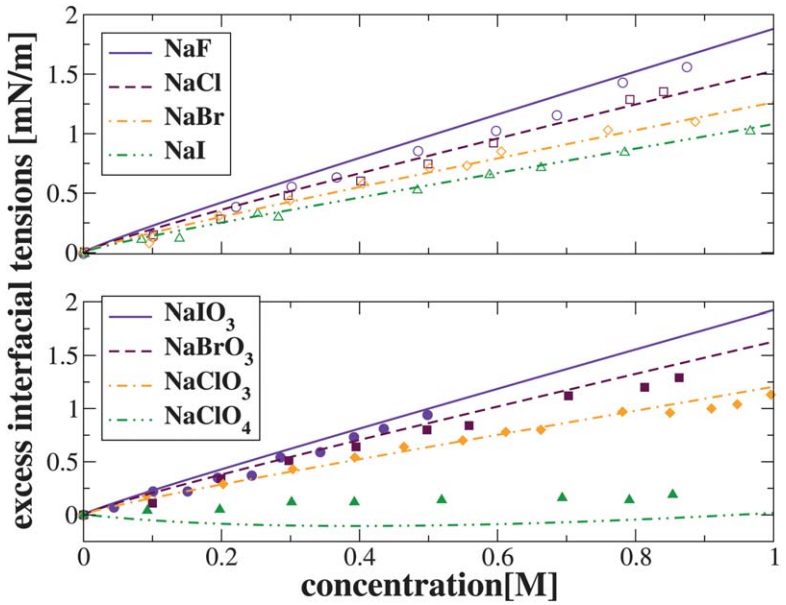

Fig. 1 Excess interfacial tensions for various salts at the electrolyte–air interface. The open circles, squares, diamonds and triangles represent experimental data[34–36] for NaF, NaCl, NaBr and NaI, respectively. The full circles, squares, diamonds and triangles represent experimental data[36] for $NaIO_3$, $NaBrO_3$, $NaClO_3$ and $NaClO_4$, respectively. The lines represent the present theory.

to its crystallographic size. The calculated excess surface tension for all halide salts are in excellent agreement with the experimental measurements, Fig. 1.

At the moment there is no general theory for ionic hydration. For halide anions we saw that there was a very good correlation between the size of the ion, its JD viscosity *B*-coefficient, and the hydration characteristics near the air–water interface. One might hope that such correlations will also persist for more complicated anions as well. This, however, is not the case. For example, iodate, IO_3^-, is a very large anion, yet its JD viscosity *B*-coefficient is similar to that of fluoride. Indeed, calculating the surface tension of $NaIO_3$ solution, we find that IO_3^- must be treated as a strongly kosmotropic anion. This is also consistent with the recent *ab initio* simulations of Baer *et al.*[37] Although the correlation between the ionic size and the ionic hydration is lost for more complicated oxy-anions, the correlation between the JD viscosity *B*-coefficient and the interfacial hydration seems to persist. This correlation can, therefore, be used to distinguish between the kosmotropes and the chaotropes in the case of the more complex anions.[26]

We now consider salts with oxy-anions. Although oxy-anions are not spherical, their effective radii are well described by an empirical formula based on experimentally measured entropies of hydration,[38] $a = \frac{n_{oxy}}{4}(d + 1.4/\text{Å})$,where n_{oxy} is the number of oxygens in the anion and d is the halogen–oxygen covalent bond length in the corresponding salt crystal.[33] We first consider $NaIO_3$ solution. The partially hydrated radius of sodium is the same as before, $a = 2.5$ Å. The JD viscosity *B*-coefficient[39] of IO_3^- is large and positive, 0.14. This means that iodate will remain fully hydrated near the interface, keeping its bulk hydration radius[33] $a = 3.74$ Å. The ion-interface potential of IO_3^- is then $U_-(z) = U_f(z)$, with a hardcore repulsion at $z = 3.74$ Å from the GDS. Calculating the excess surface tension for $NaIO_3$, we find a good agreement with experiment, Fig. 1. The ion BrO_3^- has the *B*-coefficient[39]

near zero, 0.009, similar to Cl^- so, once again, we will treat these ion as a kosmotrope with a partially hydrated radius equal to its bare size $a = 2.41$ Å. The result of this calculation is shown in Fig. 1. The ions ClO_3^- and ClO_4^- have negative B coefficients,[39] −0.022 and −0.058, respectively, and are chaotropes. The total ion–interface interaction potential for these ions is $U_-(z) = U_i(z) + U_p(z) + U_c(z)$, with bare ionic radii,[38] $a = 2.16$ and $a = 2.83$ Å; and relative polarizabilities,[26,32] $\alpha = 0.52$ and $\alpha = 0.24$, respectively. The calculated excess interfacial tension for $NaClO_3$ agrees very well with the experimental data, Fig. 1. The agreement is not very good for sodium perchlorate, Fig. 1. This ion is very big, so that a small error in its effective radius calculated using the empirical formula presented above leads to a large error in its cavitational free energy—cavitational energy scales with the cube of the radius—resulting in an incorrect estimate of adsorption. The theory also allows us to estimate the electrostatic potential difference across the interface,[26] $\phi(\infty) - \phi(0)$, which is reported in Table 1 for various salts at 1 M concentration. The results are in a qualitative agreement with the experimental measurements of Frumkin[40] and Jarvis and Scheiman.[41] Furthermore, if the ions are arranged in the order of increasing surface potential, one finds precisely the celebrated Hofmeister series.[26]

Acids solutions

While most salts tend to increase the surface tension of the air–water interface, most acids do precisely the opposite. It is well known that proton H^+ interacts strongly with the water molecules,[43–45] forming complexes such as H_3O^+ and $H_2O_5^+$. The trigonal pyramidal structure of hydronium[46,47] favors strong adsorption at the water–air interface, with the oxygen pointing towards the air.[17,46–49] For many acids the protonation of the interface is so strong as to result in a negative excess surface tension. To take this into account[50] we add an additional adsorption potential for H^+,

$$\beta U_h(z) = \begin{cases} 0 \text{ for } z \geq 1.97\text{Å}, \\ -3.05 \text{ for } z < 1.97\text{Å}. \end{cases} \quad (8)$$

where the value −3.05 was adjusted in order to obtain the correct excess interfacial tension for the hydrochloric acid, Fig. 2. The range of this potential is taken to be 1.97 Å, the length of the hydrogen bond. The anions are treated as before—classified as kosmotropes or chaotropes[50]—while the proton interacts with the interface through the potential $U_+(z) = U_i(z) + U_h(z)$. In the image part of this potential the radius of a proton is set to zero.

Table 1 Surface potentials difference at 1 M for various salts

Salts	Calculated/mV	Frumkin/mV40,42	Jarvis *et al.*/mV41
NaF	4.7	—	—
NaCl	−2.1	−1	≈−1
NaBr	−9.4	—	≈−5
NaI	−14.3	−39	≈−21
$NaIO_3$	5	—	—
$NaBrO_3$	−0.12	—	—
$NaNO_3$	−8.27	−17	≈−8
$NaClO_3$	−11.02	−41	—
$NaClO_4$	−31.1	−57	—
Na_2CO_3	10.54	3	≈6
Na_2SO_4	10.17	3	≈35

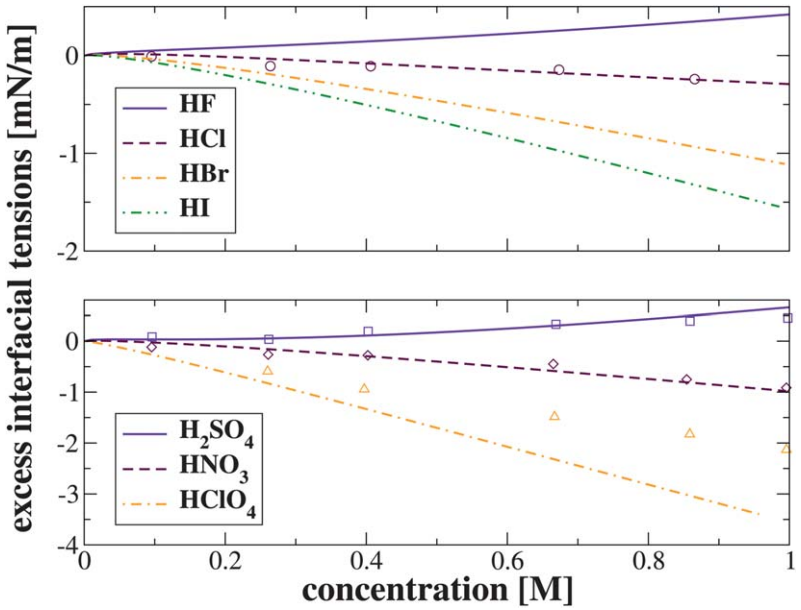

Fig. 2 Excess interfacial tensions for various acids at the electrolyte–air interface. The open circles, squares, diamonds and triangles represent experimental data[51] for HCl, H_2SO_4, HNO_3 and $HClO_4$, respectively. The lines represent the present theory.

In Fig. 2 the excess interfacial tensions for various acids are plotted. The agreement with the experimental data is very good for H_2SO_4 and HNO_3. As for sodium perchlorate, $HClO_4$ also shows a significant deviation from the experimental data, indicating again that our estimate of the effective radius of ClO_4^- is too large.

To calculate the electrostatic potential difference across the interface we integrate the PB equation. This, however, will not account for the reorientation of the interfacial water molecules when hydronium complex is formed, resulting in a dipole layer with a corresponding potential drop.[52] As was discussed earlier H_3O^+ prefers to orient itself with the hydrogens pointing towards the bulk water. The number of hydroniums formed can be estimated from the proton adsorption, $N_+ = [N - V\rho_+(0)]$, where $\rho_+(0)$ is the bulk concentration, given by eqn (2). The internal electric field inside the dipole layer can be estimated to be $E = 4\pi pN_+/\varepsilon_o Sd$, where $p = 0.3854q$ Å the water dipole moment, d is the dipole length, and S is the interfacial area. Integrating this field across the interface, we find the contribution of the surface hydroniums to the overall potential difference across the interface to be $\Delta\phi_w = -69604.5\Gamma_+$, in mV. Summing this with the contribution arising from the PB equation, we obtain the overall potential drop across the air–water interface,

Table 2 Electrostatic potential differences across the water–air interface for various acids (including the contributions from PB equation and the oriented water dipoles)

Acids	calculated/mV	Frumkin/mV40
HF	85.5	−71
HCl	1.24	−23
HNO_3	−84.4	−48
HBr	−95	−34
HI	−144.8	−61
$HClO_4$	−412	−82

reported in Table 2. The theoretical results are also compared with the data of Frumkin.[40] In view of the roughness of the estimates presented above the qualitative agreement between the theory and experiment is quite reasonable. The value −71mV for HF reported in ref. 40 most like has as a wrong sign, since it falls completely outside the general trend.

Electrolyte–oil interface

The good agreement between the theory and experiments suggests that the physical picture behind the mechanism of the ion–interface interaction presented above is more-or-less correct. In particular we see that the ions near the air–water interface must be divided into two classes: kosmotropes and chaotropes.[26] While the kosmotropes remain hydrated near the interface the chaotropes lose their hydration shell and, as the result of the hydrophobic cavitational forces and high polarizability, become partially adsorbed to the interface. In their recent *ab initio* simulations, Baer and Mundy[53] have calculated the potential of mean force for iodide near the air–water interface, finding an almost perfect agreement with the theory presented above.[23] This suggests that the dispersion (van der Waals) interactions do not play a significant role at the air–water interface. To see why this might be the case, let us first consider a kosmotropic ion. Near the interface, such an ion remains fully hydrated, interacting with almost the same number of water molecules as in the bulk, so that the dispersion contribution to its total free energy of solvation should not be affected by the presence of the interface.

For chaotropic ions, the absence of dispersion interactions is not so easily understood. It is possible, however, to make the following argument: most of the ionic charge of a chaotropic anion as it crosses the GDS concentrates in water, resulting in a large electric field.[23] This strong field attracts water molecules so that it is possible for a chaotropic ion to interact dispersively with the same number of water molecules as it did in the bulk. To see if this argument is consistent, we will now study the effect of electrolyte on the interfacial tension of the oil–water interface.

Similar to what happens at the air–water interface, the kosmotropic ions near the oil–water interface will feel the ion–image interaction and the hardcore repulsion from the GDS. Oil, like air, has low dielectric constant, $\varepsilon_o \approx 2$, so that the ion-image and the polarization potentials, eqn (3) and (5), will remain the same as at the air–water interface. The chaotropic ions are driven towards the interface by their cavitational potential. When part of the ion penetrates into oil, there is also a cavitation energy penalty from the oil side. The cavitational energy, is mostly entropic—related to the number of water/oil molecules excluded from the cavity produced by the ion. The molecular weight of oil (dodecane used in the experiments) is 10 times higher, while its mass density is the same as that of water. This means that the number of excluded molecules in the ion cavity, and consequently the cost of cavitational energy, in oil will be about 10 times smaller than in water, and can be safely neglected. Therefore, the cavitational potential of a chaotrope at the water–oil interface will remain the same as at the air–water interface, eqn (7).

Since at the air–water interface there is no dispersive contribution to the adsorption potential, the dispersion interaction with the oil–water interface should be proportional to the ionic polarizability and the ionic volume exposed to oil. We, therefore, suggest the following simple phenomenological expression[54]

$$U_d(z) = \begin{cases} 0 \text{ for } z \geq a, \\ A_{\text{eff}}\alpha\left[1 - \dfrac{(z/a+1)^2(2-z/a)}{4}\right] \text{for } -a < z < a, \end{cases} \quad (9)$$

where A_{eff} is the effective Hamaker constant, $A_{\text{eff}} \approx A^v_{\text{mw}} - A^v_{\text{mo}}$, where A^v_{mw} and A^v_{mo} are the metal–water and metal–oil (dodecane) Hamaker constants in vacuum.[54] The

metal constants are used since the ionic polarizability is already included in eqn (9). Using the tabulated values of the Hamaker constants, from ref. 55, we obtain $A_{\text{eff}} \approx -4k_{\text{B}}T$. Note that this is only a rough estimate of the strength of the dispersion interaction. In practice, we will adjust the value of A_{eff} to obtain the measured interfacial tension of the KI solution.

The excess interfacial tensions will be calculated as before. We will solve the modified PB equation eqn (2) inside the drop with potentials: $U_+(z) = U_i(z)$ for K^+, $U_-(z) = U_i(z)$ for kosmotropes, and $U_-(z) = U_i(z) + U_p(z) + U_c(z) + U_d(z)$ for chaotropes. From this solution we will calculate the ionic adsorption and, integrating the Gibbs adsorption isotherm eqn (1), will obtain the interfacial tensions. All the parameters used for the kosmotropes and the chaotropes are the same as in the previous sections. The hydrated radius of the K^+ is adjusted to obtain the experimentally measured surface tension of KCl solution, Fig. 3. We find that the potassium ion is partially hydrated with radius of $a = 2$ Å. This radius will be used for all the potassium salts. To obtain the effective Hamaker constant for chaotropic ions, we study the KI solution, Fig. 3. Fitting the experimental data we obtain $A_{\text{eff}} = -4.4k_{\text{B}}T$, which is in excellent agreement with our theoretical estimate, suggesting that our physical picture about the role of dispersion interactions at the air–water and oil–water interfaces is correct. This Hamaker constant will be used for all the chaotropic anions. In Fig. 3, we present the calculated interfacial tensions for various potassium salts. The only additional experimental data available to us is for KBr, which agrees very well with the predictions of the present theory.

Acids–oil interface

We will now explore the effect of acids on the interfacial tension of the water–oil interface. It was shown previously that the hydronium ion H_3O^+ has a particular preference for the interfacial solvation. This happens because the hydrogens of the

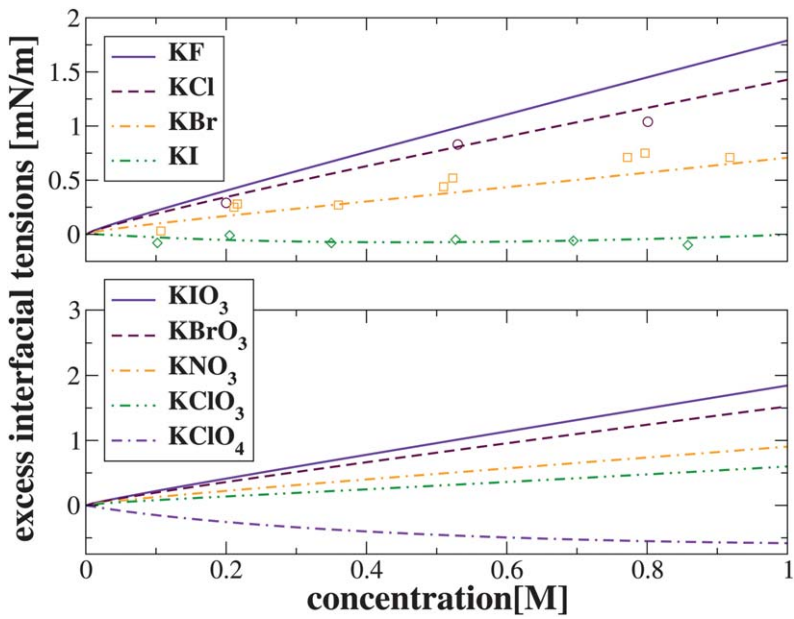

Fig. 3 Excess interfacial tensions for various electrolyte solutions. The open circles, squares and diamonds represent experimental data[56] for KCl, KBr and KI, respectively. The lines are calculated using the present theory.

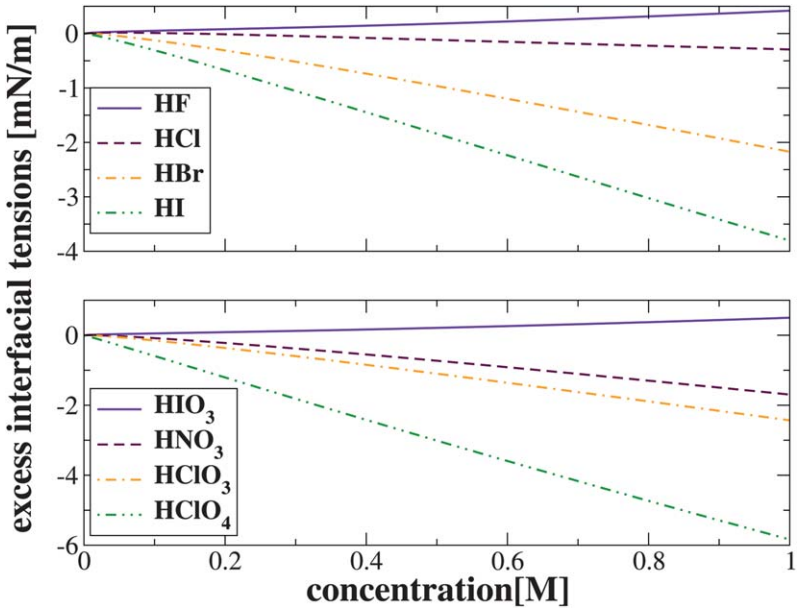

Fig. 4 Excess interfacial tensions for different acids. The lines are calculated using the present theory.

hydronium ion are very good hydrogen bond donors, while the oxygen is a bad receptor.[46] This leads to a preferential orientation of the hydronium ion at the water–air interface, with the hydrogens pointing into the aqueous environment and the oxygen sticking out. Calculations of solvation free energy confirm this interfacial behavior.[57] Here we will suppose that this basic picture persists for hydronium ion at the water–oil interface as well. Since at the moment there are no experimental measurements of the interfacial tension of acid solutions which could be used to re-parameterize our model, we will use the same adsorption energy of proton as at the air–water interface,[50] $-3.05\ k_{\mathrm{B}}T$. The dispersion interaction and the cavitational potential are also the same as used in the previous sections. Integrating the modified PB equation and the Gibbs adsorption isotherm, we obtain the ionic adsorption and the excess interfacial tensions of different acids. In Fig. 4 we present our results. A significant decrease in the pure water–oil interfacial tension is observed for acids containing chaotropic anions. Unfortunately at the moment there is no experimental data available to test the predictions of the present theory.

The theory can also be used to estimate the electrostatic potential across the acid–oil interface. The calculation is analogous to the one performed for the acid–air interface.[50] The results are presented in Table 3. It is very probable that the

Table 3 Electrostatic potential differences across the oil–water interface for various acids (including the contributions from PB equation and the oriented water dipoles)

Acids	Calculated/mV
HNO_3	−154.53
HBr	−196.67
$HClO_3$	−218.36
HI	−320.65
$HClO_4$	−453.78

calculated potential differences are too large, since the theory is not fully self-consistent. Nevertheless the results provide us with a magnitude of the electrostatic potential difference that can be expected across the water–oil interface for different acids.

Conclusions

We have presented a general theory which allows us to calculate the surface and the interfacial tensions of electrolyte solutions. The theory provides a very interesting picture of ionic specificity. We find that near the air–water interface or a general hydrophobic surface, ions can be divided into two classes: kosmotropes and chaotropes.[5,26] Near the interface kosmotropes remain hydrated and are repelled from the GDS. On the other hand, chaotropes lose their hydration sheath and, as a result of large polarizability, can become adsorbed to the hydrophobic interface. The theory also shows that the hydronium ion has a strong preference for interfacial solvation.[50]

It is believed that the surface water molecules are preferentially oriented with the hydrogens sticking out towards the air. To account for the measured electrostatic potential difference of acid solutions, we find that hydronium must orient itself opposite to the surface water, with its hydrogens pointing toward the bulk.[52]

Beyond a qualitative picture, the theory presented in this paper allows us to make quantitative predictions about the surface and the interfacial tensions of electrolyte and acid solutions as well as to calculate the electrostatic potential difference across the interface. The theory can also be extended to calculate quantitatively the critical coagulation concentrations of hydrophobic colloidal suspensions, providing a new insight into the physical mechanisms responsible for the ionic specificity.[5]

Although the theory helps us to understand the physics behind the Hofmeister series, there are still a number of issues that must be explored. One of them is the role of the electrostatic surface potential of water. The dielectric continuum theory presented in this paper completely ignores the surface potential of water, suggesting that it should be negligibly small. This is justified *a posteriori* by the good agreement between the theory and the experimental measurements of the surface and the interfacial tensions of acids and electrolytes. On the other hand, the classical point charge water models[58–60] predict that across the air–water interface there should be an electrostatic potential drop of approximately −600 mV. If such surface potential really exists, it would completely change the electrostatics of ionic solvation, favoring a much stronger adsorption of the chaotropic anions than is predicted by the present theory. This, however, cannot be true since a stronger adsorption would result in an erroneous surface tensions of electrolyte solutions! In fact, it is now believed that the polarizable force field simulations, which have stimulated the development of the present theory, lead to too much adsorption of the chaotropic anions. We speculate that the reason for this excessive adsorption is precisely the artificial surface potential of the point charge water models.

If the existing classical water models cannot account for the surface properties of water, what about the full quantum mechanical calculations? In fact, the recent *ab initio* simulations[61–63] show that the surface potential of water is not −600 mV, but is +3000 mV. Note the difference in sign and the magnitude of this potential! The +3 V electrostatic potential difference across the air–water interface has been measured by the high energy electron holography.[58] Nevertheless, the authors of ref. 58, argue that this huge potential is irrelevant for electrochemistry. They suggest that the quantum electrostatic potential must be coarse grained on the scale of the ion. If this is done properly, they argue, the surface potential of water felt by an ion such as I^- will drop to a few mV and can be safely ignored. This is possibly the reason why the *ab initio* potential of mean force for I^- agrees so well[53] with the present dielectric continuum theory, which completely neglects the electrostatic surface potential of water. More work, however, still is necessary to fully elucidate this point.

Acknowledgements

This work was partially supported by the CNPq, FAPERGS, INCT-FCx, and by the US-AFOSR under the grant FA9550-09-1-0283.

References

1 R. Komsa-Penkova, R. Koynova, G. Kostov and B. G. Tenchov, *Biochim. Biophys. Acta, Protein Struct. Mol. Enzymol.*, 1996, **1297**, 171.
2 N. Jiang, P. X. Li, Y. L. Wang, J. B. Wang, H. K. Yan and R. K. Thomas, *J. Phys. Chem. B*, 2004, **108**, 15385.
3 L. M. Pegram, T. Wendorff, R. Erdmann, I. Shkel, D. Bellissimo, D. J. Felitsky and M. T. Record, *Proc. Natl. Acad. Sci. U. S. A.*, 2010, **107**, 7716.
4 J. M. Peula-Garcia, J. L. Ortega-Vinuesa and D. Bastos-Gonzalez, *J. Phys. Chem. C*, 2010, **114**, 11133.
5 A. P. dos Santos and Y. Levin, *Phys. Rev. Lett.*, 2011, **106**, 167801.
6 P. W. Debye and E. Hückel, *Phys. Z.*, 1923, **24**, 185.
7 I. Langmuir, *J. Am. Chem. Soc.*, 1917, **39**, 1848.
8 C. Wagner, *Phys. Z.*, 1924, **25**, 474.
9 L. Onsager and N. N. T. Samaras, *J. Chem. Phys.*, 1934, **2**, 528.
10 Y. Levin and J. E. Flores-Mena, *Europhys. Lett.*, 2001, **56**, 187.
11 M. Boström, D. R. M. Williams and B. W. Ninham, *Langmuir*, 2001, **17**, 4475.
12 A. Heydweiller, *Ann. Phys. (Leipzig)*, 1910, **33**, 145.
13 L. Perera and M. L. Berkowitz, *J. Chem. Phys.*, 1991, **95**, 1954.
14 L. X. Dang and D. E. Smith, *J. Chem. Phys.*, 1993, **99**, 6950.
15 S. J. Stuart and B. J. Berne, *J. Phys. Chem. A*, 1999, **103**, 10300.
16 P. Jungwirth and D. J. Tobias, *J. Phys. Chem. B*, 2002, **106**, 6361.
17 P. Jungwirth and D. J. Tobias, *Chem. Rev.*, 2006, **106**, 1259.
18 M. A. Brown, R. D'Auria, I. F. W. Kuo, M. J. Krisch, D. E. Starr, H. Bluhm, D. J. Tobias and J. C. Hemminger, *Phys. Chem. Chem. Phys.*, 2008, **10**, 4778.
19 D. Horinek, A. Herz, L. Vrbka, F. Sedlmeier, S. I. Mamatkulov and R. R. Netz, *Chem. Phys. Lett.*, 2009, **479**, 173.
20 G. Markovich, S. Pollack, R. Giniger and O. Cheshnovski, *J. Chem. Phys.*, 1991, **95**, 9416.
21 B. Garrett, *Science*, 2004, **303**, 1146.
22 S. Ghosal, J. Hemminger, H. Bluhm, B. Mun, E. L. D. Hebenstreit, G. Ketteler, D. F. Ogletree, F. G. Requejo and M. Salmeron, *Science*, 2005, **307**, 563.
23 Y. Levin, *Phys. Rev. Lett.*, 2009, **102**, 147803.
24 Y. Levin, A. P. dos Santos and A. Diehl, *Phys. Rev. Lett.*, 2009, **103**, 257802.
25 C. H. Ho, H. K. Tsao and Y. J. Sheng, *J. Chem. Phys.*, 2003, **119**, 2369.
26 A. P. dos Santos, A. Diehl and Y. Levin, *Langmuir*, 2010, **26**, 10778.
27 S. Rajamani, T. M. Truskett and S. Garde, *Proc. Natl. Acad. Sci. U. S. A.*, 2005, **102**, 9475.
28 Y. Marcus, *Chem. Rev.*, 2009, **109**, 1346.
29 K. D. Collins, *Biophys. J.*, 1997, **72**, 65.
30 A. W. Omta, M. F. Kropman, S. Woutersen and H. J. Bakker, *Science*, 2003, **301**, 347.
31 W. M. Latimer, K. S. Pitzer and C. M. Slansky, *J. Chem. Phys.*, 1939, **7**, 108.
32 N. C. Pyper, C. G. Pike and P. P. Edwards, *Mol. Phys.*, 1992, **76**, 353.
33 E. R. Nightingale Jr, *J. Phys. Chem.*, 1959, **63**, 1381.
34 N. Matubayasi, K. Tsunemoto, I. Sato, R. Akizuki, T. Morishita, A. Matuzawa and Y. Natsukari, *J. Colloid Interface Sci.*, 2001, **243**, 444.
35 N. Matubayasi, H. Matsuo, K. Yamamoto, S. Yamaguchi and A. Matuzawa, *J. Colloid Interface Sci.*, 1999, **209**, 398.
36 N. Matubayasi, (unpublished).
37 M. D. Baer, V. T. Pham, J. L. Fulton, G. K. Schenter, M. Balasubramanian and C. J. Mundy, *J. Phys. Chem. Lett.*, 2011, **2**, 2650.
38 A. M. Couture and K. L. Laidler, *Can. J. Chem.*, 1957, **35**, 202.
39 H. D. B. Jenkins and Y. Marcus, *Chem. Rev.*, 1995, **95**, 2695.
40 A. Frumkin, *Z. Phys. Chem.*, 1924, **109**, 34.
41 N. L. Jarvis and M. A. Scheiman, *J. Phys. Chem.*, 1968, **72**, 74.
42 J. E. B. Randles, *Advances in Electrochemistry and Electrochemical Engineering*, Interscience, New York, 1963, vol. 3, p. 1.
43 M. Eigen, *Angew. Chem., Int. Ed. Engl.*, 1964, **3**, 1.
44 G. Zundel, *Adv. Chem. Phys.*, 2000, **111**, 1.
45 D. Marx, M. E. Tuckerman, J. Hutter and M. Parrinello, *Nature*, 1999, **397**, 601.

46 M. K. Petersen, S. S. Iyengar, T. J. F. Day and G. A. Voth, *J. Phys. Chem. B*, 2004, **108**, 14804.
47 M. Mucha, T. Frigato, L. M. Levering, H. C. Allen, D. J. Tobias, L. X. Dang and P. Jungwirth, *J. Phys. Chem. B*, 2005, **109**, 7617.
48 L. M. Levering, M. R. Sierra-Hernández and H. C. Allen, *J. Phys. Chem. C*, 2007, **111**, 8814.
49 S. S. Iyengar, T. J. F. Day and G. A. Voth, *Int. J. Mass Spectrom.*, 2005, **241**, 197.
50 A. P. dos Santos and Y. Levin, *J. Chem. Phys.*, 2010, **133**, 154107.
51 P. K. Weissenborn and R. J. Pugh, *J. Colloid Interface Sci.*, 1996, **184**, 550.
52 J. E. B. Randles and D. J. Schiffrin, *Trans. Faraday Soc.*, 1966, **62**, 2403.
53 M. D. Baer and C. J. Mundy, *J. Phys. Chem. Lett.*, 2011, **2**, 1088.
54 A. P. dos Santos and Y. Levin, *Langmuir*, 2012, **28**, 1304.
55 D. B. Hough and L. R. White, *Adv. Colloid Interface Sci.*, 1980, **14**, 3.
56 R. Aveyard and S. M. Saleem, *J. Chem. Soc., Faraday Trans. 1*, 1976, **72**, 1609.
57 L. X. Dang, *J. Chem. Phys.*, 2003, **119**, 6351.
58 S. M. Kathmann, I. F. W. Kuo, C. J. Mundy and G. K. Schenter, *J. Phys. Chem. B*, 2011, **115**, 4369.
59 W. L. Jorgensen, J. Chandrasekhar, J. D. Madura, R. W. Impey and M. L. Klein, *J. Chem. Phys.*, 1983, **79**, 926.
60 L. X. Dang and T. M. Chang, *J. Chem. Phys.*, 1997, **106**, 8149.
61 S. M. Kathmann, I. F. W. Kuo and C. J. Mundy, *J. Am. Chem. Soc.*, 2008, **130**, 16556.
62 S. M. Kathmann, I. F. W. Kuo and C. J. Mundy, *J. Am. Chem. Soc.*, 2009, **131**, 17522.
63 K. J. Leung, *J. Phys. Chem. Lett.*, 2010, **1**, 496.